

hep-ex/0607041
SLAC-PUB-11856
BABAR-TALK-05/113
July 2006

Rare Decays and Search for New Physics with *BABAR*

Johannes M. Bauer
for the *BABAR* Collaboration

Abstract

Rare B decays permit stringent tests of the Standard Model and allow searches for new physics. Several rare radiative-decay studies of the B meson from the *BABAR* collaboration are described. So far no sign for new physics was discovered.

Submitted to the Conference Proceedings of the Fourth International
Conference on Frontier Science — New Frontiers in Subnuclear Physics,
September 12–17, 2005, Milan, Italy

Stanford Linear Accelerator Center, Stanford University, Stanford, CA 94309

Work supported in part by Department of Energy contract
DE-AC02-76SF00515.

Frascati Physics Series Vol. VVVVVV (xxxx), pp. 000-000
XX CONFERENCE – Location, Date-start - Date-end, Year

Rare Decays and Search for New Physics with *BABAR*

Johannes M. Bauer

University of Mississippi, University, MS 38677, U.S.A.
for the *BABAR* Collaboration

Abstract

Rare B decays permit stringent tests of the Standard Model and allow searches for new physics. Several rare radiative-decay studies of the B meson from the *BABAR* collaboration are described. So far no sign for new physics was discovered.

1 Introduction

At the SLAC PEP-II B -Factory, the *BABAR* detector collected so far more than 250M $B\bar{B}$ pairs, created by e^+e^- collisions at the $\Upsilon(4S)$ resonance. This data set makes searches for rare decays feasible at branching fractions (BF) of 10^{-4} or less. This talk concentrates on radiative B decays. Additional results from *BABAR* were discussed elsewhere at this conference. ¹⁾

2 Fully- and Semi-inclusive $B \rightarrow X_s \gamma$, $B \rightarrow K^*(892)\gamma$ & $B \rightarrow K_2^*(1430)\gamma$

The lowest-order Feynman diagram of $b \rightarrow s \gamma$ is a one-loop electromagnetic penguin, in which non-Standard Model (non-SM) virtual particles (like the Higgs) might influence the decay rate. Measuring the energy distribution of the b quark inside the B meson helps extract $|V_{ub}|$ from $B \rightarrow X_{ul} \nu$. The decay $b \rightarrow s \gamma$ was studied in inclusive and exclusive modes using $\sim 89\text{M } B\bar{B}$ pairs.

In the so-called “fully-inclusive” measurement only the photon of $B \rightarrow X_s \gamma$ needs to be detected, but large background has to be suppressed. In the “semi-inclusive” measurement, the $B \rightarrow X_s \gamma$ BF is determined from 38 exclusive states with about 45% of the total rate estimated to be missing.

The E_γ spectra from the two $B \rightarrow X_s \gamma$ analyses are shown in Fig.1. The $K^* \gamma$ peak, prominent at high E_γ for the semi-inclusive analysis, is not visible for the inclusive analysis due to resolution constraints. Fig.2 left plots the fully-inclusive partial BFs against the value of the lower cut in E_γ . The overall semi-inclusive BF, when extrapolated to $E_\gamma > 1.6 \text{ GeV}$, agrees with the SM prediction and with the results from other experiments (Fig.2 right). 2, 3)

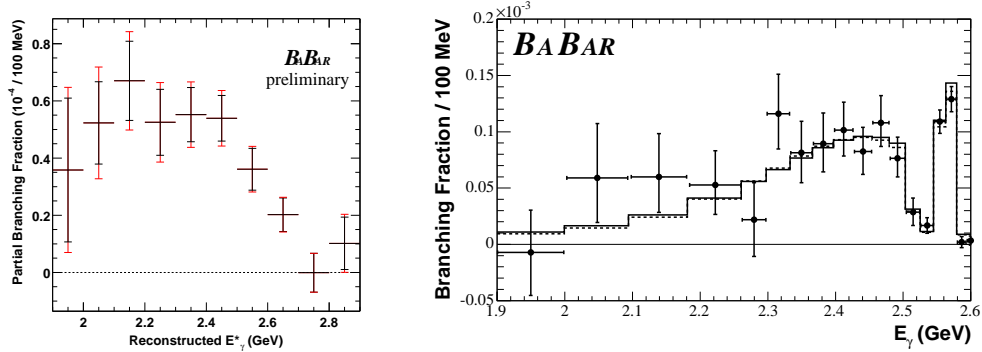


Figure 1: *Photon energy spectrum from fully- (left, in $\Upsilon(4S)$ frame) and semi-inclusive $B \rightarrow X_s \gamma$ analyses (right, in B frame, with theory spectra overlaid).*

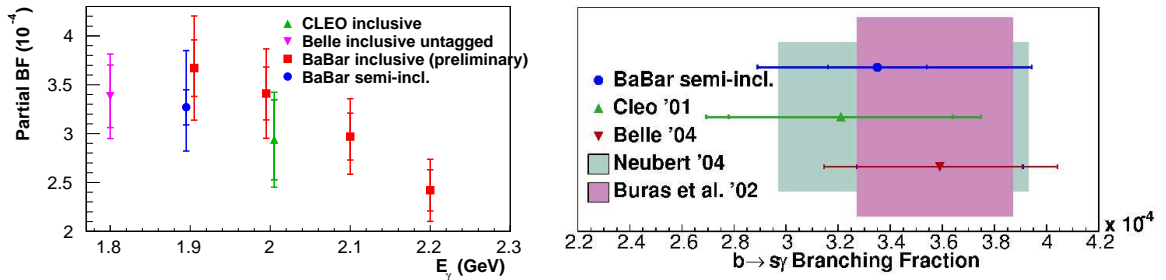


Figure 2: *Partial BFs versus lower cut in E_γ (left) and overall BF measurements (right) of $B \rightarrow X_s \gamma$ for $E_\gamma > 1.6 \text{ GeV}$.*

Non-perturbative hadronic effects complicate the theoretical calculations of exclusive decays like $B \rightarrow K^*(892)\gamma$ and $B \rightarrow K_2^*(1430)\gamma$, so that the measurements are currently more accurate than the predictions. A summary of the results is shown in Fig.3. 4, 5)

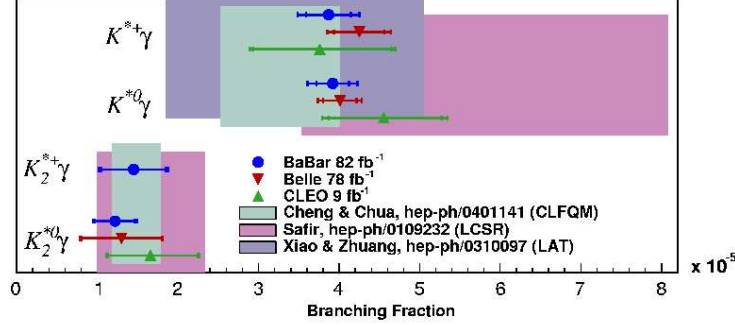


Figure 3: Branching fractions of $B \rightarrow K^*(892)\gamma$ and $B \rightarrow K_2^*(1430)\gamma$.

3 $B \rightarrow X_s ll$, $B \rightarrow K^{(*)}ll$ and $B \rightarrow (\rho, \omega)\gamma$

The decay $b \rightarrow sll$ has been measured semi-inclusively ($B \rightarrow X_s ll$) on 89M $B\bar{B}$ pairs, and exclusively ($B \rightarrow K^{(*)}ll$) on 229M $B\bar{B}$ pairs. The former measurement is again based on a sum of exclusive states, with about half of the total rate missing, and its BF ⁶⁾ of $(5.6 \pm 1.5 \pm 0.6 \pm 1.1) \times 10^{-6}$ for $m_u > 0.2 \text{ GeV}/c^2$ agrees well with the SM prediction. The exclusive decay results are shown in Fig.4 left. ⁷⁾

The decay $b \rightarrow d\gamma$ has been studied in 221M $B\bar{B}$ pairs by searching for $B \rightarrow (\rho, \omega)\gamma$. These decays go primarily through penguin diagrams, but also through W -exchange or W -annihilation. The background originates mainly from $q\bar{q}$ ($=udsc$) events. The BF results are summarized in Fig.4 right. ⁸⁾

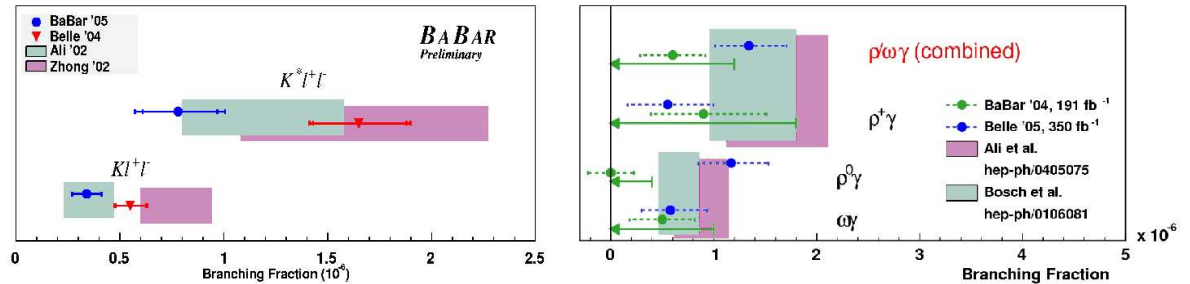


Figure 4: BF measurements and SM predictions for $K^{(*)}ll$ (left) and $B \rightarrow (\rho, \omega)\gamma$ decays (right).

4 $\bar{B}^0 \rightarrow D^{*0}\gamma$ and $B^0 \rightarrow \phi\gamma$

The $\bar{B}^0 \rightarrow D^{*0}\gamma$ decay with SM predictions around 10^{-6} is dominated by W -exchange. The final B candidates from 88M $B\bar{B}$ pairs are described by $m_{\text{ES}} = \sqrt{E_{\text{beam}}^{*2} - p_B^{*2}}$ and $\Delta E^* = E_B^* - E_{\text{beam}}^*$, with E_{beam}^* being the center-of-mass (CM) beam energy, and E_B^* and p_B^{*2} the B candidate's CM energy and momentum. Background, mainly from $B\bar{B}$ decays, is estimated to be 9.4 ± 1.7 events in the $m_{\text{ES}}-\Delta E$ signal box. Thirteen observed data events (Fig.5 left) lead to a BF upper limit of 2.5×10^{-5} at 90% confidence level (CL).⁹⁾

The experimental signature of the $B^0 \rightarrow \phi\gamma$ decay is clean, but the SM prediction of the BF is very low with 3.6×10^{-12} . Candidates are selected from 124M $B\bar{B}$ pairs. In the signal region, a $q\bar{q}$ ($B\bar{B}$) background of 6.0 ± 1.0 (<0.1) events is expected. Eight events observed in data (Fig.5 right) result in a BF upper limit of 8.5×10^{-7} at 90% CL.¹⁰⁾

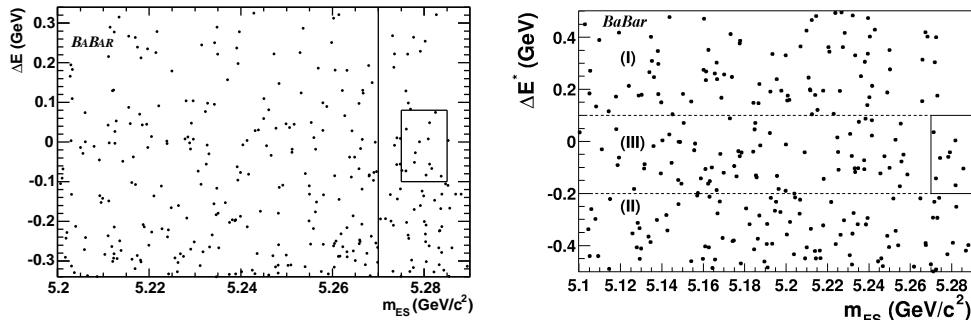


Figure 5: $m_{\text{ES}}-\Delta E$ plane of real data for $\bar{B}^0 \rightarrow D^{*0}\gamma$ (left) and $B^0 \rightarrow \phi\gamma$ (right). In both plots the signal box is indicated on the right side.

The author thanks the *BABAR* collaboration, the SLAC accelerator group and all contributing computing organizations. He was supported by U.S. Department of Energy grant DE-FG05-91ER40622.

References

1. Presentations by Fernando Ferroni and Gagan Mohanty this conference.
2. *BABAR* Collaboration, B. Aubert *et al.*, hep-ex/0507001 (2005).
3. *BABAR* Collaboration, B. Aubert *et al.*, Phys. Rev. D **72**, 052004 (2005).
4. *BABAR* Collaboration, B. Aubert *et al.*, Phys. Rev. D **70**, 112006 (2004).
5. *BABAR* Collaboration, B. Aubert *et al.*, Phys. Rev. D **70**, 091105 (2004).
6. *BABAR* Collaboration, B. Aubert *et al.*, Phys. Rev. Lett. **93**, 081802 (2004).
7. *BABAR* Collaboration, B. Aubert *et al.*, hep-ex/0507005 (2004).
8. *BABAR* Collaboration, B. Aubert *et al.*, Phys. Rev. Lett. **94**, 011801 (2005).
9. *BABAR* Collaboration, B. Aubert *et al.*, Phys. Rev. D **72**, 051106 (2005).
10. *BABAR* Collaboration, B. Aubert *et al.*, Phys. Rev. D **72**, 091103 (2005).